



An ultra-sensitive capacitive microwire sensor for pathogen-specific serum antibody responses

Lei Wang^a, Jessica E. Filer^{b,c}, Meghan M. Lorenz^c, Charles S. Henry^{a,d}, David S. Dandy^{a,e,*}, Brian J. Geiss^{a,c,*}

^a School of Biomedical Engineering, Colorado State University, Fort Collins, CO 80523, USA

^b Cell and Molecular Biology Program, Colorado State University, Fort Collins, CO 80523, USA

^c Department of Microbiology, Immunology, and Pathology, Colorado State University, Fort Collins, CO 80523, USA

^d Department of Chemistry, Colorado State University, Fort Collins, CO 80523, USA

^e Department of Chemical and Biological Engineering, Colorado State University, Fort Collins, CO 80523, USA

ARTICLE INFO

Keywords:

Capacitive affinity biosensor
Microwires
Antibody detection
Isotype
Zika virus
Mouse serum

ABSTRACT

Detection of viral infection is commonly performed using serological techniques like the enzyme-linked immunosorbent assay (ELISA) to detect antibody responses. Such assays may also be used to determine the infection phase based on isotype prevalence. However, ELISAs demonstrate limited sensitivity and are difficult to perform at the point of care. Here, we present a novel technique for label-free, rapid detection of ultra-low concentrations of virus specific antibodies. We have developed a simple, robust capacitive biosensor using microwires coated with Zika or Chikungunya virus envelope antigen. With little discernable nonspecific binding, the sensor can detect as few as 10 antibody molecules in a small volume (10 molecules/30 μ L) within minutes. It can also be used to rapidly, specifically, and accurately determine the isotype of antigen-specific antibodies. Finally, we demonstrate that anti-Zika virus antibody can be sensitively and specifically detected in dilute mouse serum and can be isotyped using the sensor. Overall, our findings suggest that our microwire sensor platform has the potential to be used as a reliable, sensitive, and inexpensive diagnostic tool to detect immune responses at the point of care.

1. Introduction

Analyzing the humoral antibody response in clinical samples is critical to diagnose infectious disease, understand pathogenesis and immune response kinetics, and develop vaccines, and the enzyme-linked immunosorbent assay (ELISA) is used as the gold standard clinical diagnostic tool for antibody detection (Crowther, 2008). However, ELISAs require large instrumentation in centralized laboratories and specialized training to execute and interpret the results (Baden et al., 2016) which limits the utility of ELISAs in low-resource settings (Rabe et al., 2016). Many cases therefore go undiagnosed which indicates an urgent need for sensitive, robust assays that quickly diagnose infection at point of care (POC) and provide health-care providers with actionable information. While lateral flow assays are promising candidates for POC applications, these assays often lack sensitivity and demonstrate interference from matrix components of unprocessed samples (Posthuma-Trumpie et al., 2009).

Capacitive biosensors employ direct sample application for label-

free detection. Other electrochemical antibody sensors have been developed for serological analysis, but these designs incorporate enzymatic labels (Adornetto et al., 2015; Prado et al., 2018) or redox couples (Cabral-Miranda et al., 2018) that increase complexity and cost. Compared to other immunosensors, capacitive biosensors are ideal candidates for sensitive and label-free bioanalysis platforms. Capacitive sensing is based on the theory of the electrical double layer (DL) (Ertürk and Mattiasson, 2017; Berggren et al., 2001), where the working electrode is conjugated with probe that binds a target to increase the length of the DL. Because capacitance is inversely proportional to the DL length, this increase produces a corresponding decrease in capacitance. Such capacitive signals provide a direct, rapid measure of target binding. Based on our previous work using capacitance to detect DNA (Wang et al., 2016), the sensitivity of capacitive biosensors is far superior to traditional diagnostic assays (Loyprasert et al., 2010; Mattiasson and Hedström, 2016) and is ideal to detect low antibody titers during early stages of infection. Capacitive biosensors are thus an attractive sensing modality that has not yet been fully explored for

* Corresponding authors at: Department of Chemical and Biological Engineering, Colorado State University, Fort Collins, CO 80523, USA.

E-mail addresses: David.Dandy@colostate.edu (D.S. Dandy), Brian.Geiss@colostate.edu (B.J. Geiss).

<https://doi.org/10.1016/j.bios.2019.01.040>

Received 22 August 2018; Received in revised form 17 January 2019; Accepted 21 January 2019

Available online 29 January 2019

0956-5663/ © 2019 Elsevier B.V. All rights reserved.

specific antibody detection.

The goal of this work is to develop a novel POC platform that can specifically detect low levels of antibodies in serum. Due to its clinical relevance, Zika virus (ZIKV) was chosen as a model system to validate the platform. ZIKV is an emerging Flavivirus that is closely related to other mosquito-borne viruses like yellow fever, West Nile, and dengue. It recently became a major public health concern due to neurological complications in infected adults (Mécharles et al., 2016; Carteaux et al., 2016; Oehler et al., 2014; Soares et al., 2016) and severe developmental complications for fetuses of infected women (van der Eijk et al., 2016; Mlakar et al., 2016; Leal et al., 2016; Ventura et al., 2017, 2016). Therefore, accurate and early diagnosis of ZIKV is essential for proper monitoring and medical intervention in these cases.

In this study, we developed a capacitive immunosensor that specifically detects ZIKV and Chikungunya (CHIKV) antibodies using a sensor modified with their respective envelope (E) protein. It directly measures monoclonal antibody with a lower boundary of approximately 10 antibody molecules in a 30 μ L sample. The antibody detection system discriminates between antibodies with little cross-reactivity and can even differentiate isotypes, indicating marked selectivity. We also demonstrate that our system can specifically and sensitively detect polyclonal anti-ZIKV antibodies present in mouse serum. This method is distinguished from previous antibody detection methods not only in the platform, but also by its superior sensitivity and specificity.

2. Material and methods

2.1. Study design

The working microwire surface was functionalized with E protein from either ZIKV (ZIKV E) or Chikungunya virus (CHIKV E). Lower dynamic range boundaries for the device were first determined with monoclonal antibody samples. Anti-ZIKV E antibody was employed as a specific target while anti-CHIKV E, anti-Dengue, and anti-M13 were used as nonspecific targets. The microwire biosensor was also used to isotype the monoclonal antibodies with anti-mouse IgG1, IgG2a, IgG2b, IgG3, IgA and IgM antibodies. The microwire sensor was then validated using pre-immune and immune mouse sera collected 4, 7, 14 and 21 days post-ZIKV immunization. Next, the sensor was used to isotype Day 4 and 21 mouse sera for IgM and IgG.

Information for immunization and sera characterization, electrode functionalization and sensor fabrication are described in [Supplemental Information](#). Representative serum samples positive for ZIKV IgG antibody by Western blot were included in the serum testing. Control samples and experimental sample replicates are indicated in the text and figure legends.

2.2. Materials and equipment

Potassium hydroxide (KOH), iron (III) chloride hexahydrate ($\text{FeCl}_3 \cdot 6\text{H}_2\text{O}$), 30% hydrogen peroxide (H_2O_2), and absolute ethanol were purchased from Fisher Scientific (Fairlawn, NJ). High-purity silver ink was purchased from SPI Supplies (West Chester, PA). 11-Mercaptoundecanoic acid (MUA) was purchased from Santa Cruz Biotechnology (Dallas, TX). 3-Mercapto-1-propanol (MPOH) was purchased from Tokyo Chemical Industry Co., Ltd. (Portland, OR). N-Hydroxysuccinimide (NHS) and 1-Ethyl-3-(3-dimethylaminopropyl)-carbodiimide (EDC) were purchased from Acros Organics (Geel, Belgium). Ethanolamine, Tween-20, and 2-(N-morpholino) ethanesulfonic acid (MES) was purchased from Sigma-Aldrich (St. Louis, MO). Phosphate buffered saline ($1 \times \text{PBS}$: 137 mM NaCl, 2.7 mM KCl, 10 mM Na_2HPO_4 and 1.8 mM KH_2PO_4 , pH 7.4) was purchased from Hyclone (Logan, UT). All reagents were used as received without further purification. All stock solutions were prepared using ultrapure water (18 M Ω cm) purified with the Nanopure System (Kirkland, WA). Wires of 99.99% pure gold (25 μ m) and silver (25 μ m) were purchased from

California Fine Wire Company (Grover Beach, CA) and used as the working and reference electrode materials, respectively.

Recombinant ZIKV E, recombinant CHIKV E, and mouse monoclonal anti-CHIKV E antibodies were purchased from MyBioSource, Inc. (San Diego, CA) and stored at -20°C until use. M13 antibody (Abcam ab24229), anti-dengue 2 envelope antibodies (Abcam ab80914), and ZV-2 Anti-Zika envelope antibody (Miner et al., 2016) were generously provided by Dr. Michael Diamond. The concentration of ZIKV and CHIKV monoclonal antibodies was validated using a Nanodrop 2000c spectrophotometer from Thermo Scientific (Waltham, MA). ZIKV immune mouse serum was generated after DNA immunization of mice with ZIKV virus-like particle expression plasmids modeled from previous work (Pierson et al., 2006). Details for the construction of the immunization plasmids, immunization, serum collection, and initial antibody testing of serum are found in [Supplemental Information](#). Anti-Mouse IgG1, IgG2a, IgG2b, IgG3, IgG, IgA and IgM antibodies were purchased from BD Biosciences (San Jose, CA), and stored at 4°C until use.

2.3. Capacitance measurement device and setup

The working electrode functionalization and sensor fabrication protocols are described in the [Supplementary Information](#). Capacitance measurements were collected using an Instek LCR-821 benchtop LCR meter (New Taipei City, Taiwan) with a PC interface for data acquisition. Because DL capacitance is a non-Faradaic signal, a 0 V DC bias voltage was applied. A 20 mV root mean square (RMS) AC voltage was applied to the sensors at 20 Hz. All capacitance readouts were recorded in parallel mode in 30 μ L of $0.1 \times \text{PBST}$ and 60 data points were collected per reading. A Faraday cage was used to remove electrical interference during readout. Capacitance data was analyzed using Matlab (Mathworks) and statistical tests were performed using R (www.r-project.org). Only p values less than 0.05 were considered statistically significant.

2.4. Monoclonal antibody and isotype detection

For all antibody detection studies, a 30 μ L dilution of monoclonal antibody was added to the well and incubated for 5 min at room temperature in $1 \times \text{PBST}$ buffer containing ~ 1 to $\sim 10^3$ molecules of each monoclonal antibody. The 5 min incubation time was selected by monitoring the rate of signal change; in all experiments, sufficient signal to noise was obtained. Additional discussion regarding incubation time may be found in [Supplemental Information](#). Following incubation, electrodes were rinsed three times first with $1 \times \text{PBST}$ buffer to remove residual protein and then again three times with $0.1 \times \text{PBST}$ buffer to remove excess salts that may interfere with electrochemical readout. For isotype determination, 30 μ L of monoclonal CHIKV E antibody was added to the well and incubated for 5 min at room temperature in $1 \times \text{PBST}$ buffer. Electrodes were rinsed with $1 \times$ and $0.1 \times \text{PBST}$, and antibodies against each isotype were added to the well at dilutions of ~ 1 to $\sim 10^3$ in $1 \times \text{PBST}$ buffer. Electrodes were then rinsed again three times with 30 μ L $1 \times \text{PBST}$ buffer and 30 μ L $0.1 \times \text{PBST}$ buffer. Capacitance measurements were performed as described in the [Section 2.3](#).

2.5. Mouse serum sample antibody and isotype detection

Clarified mouse sera were diluted 1:10⁶ and 1:10¹² in 30 μ L of $1 \times \text{PBST}$ buffer and incubated on microwire chips for 5 min at room temperature. Following incubation, electrodes were rinsed three times with 30 μ L $1 \times \text{PBST}$ buffer and three times with 30 μ L $0.1 \times \text{PBST}$ buffer. To determine the isotype of anti-ZIKV antibodies in the mouse sera the microwire sensor was first immersed in 30 μ L of mouse serum diluted 1:10⁶ in $1 \times \text{PBST}$ for 5 min at room temperature. Antibodies specific for each isotype were then incubated for 5 min at dilutions of

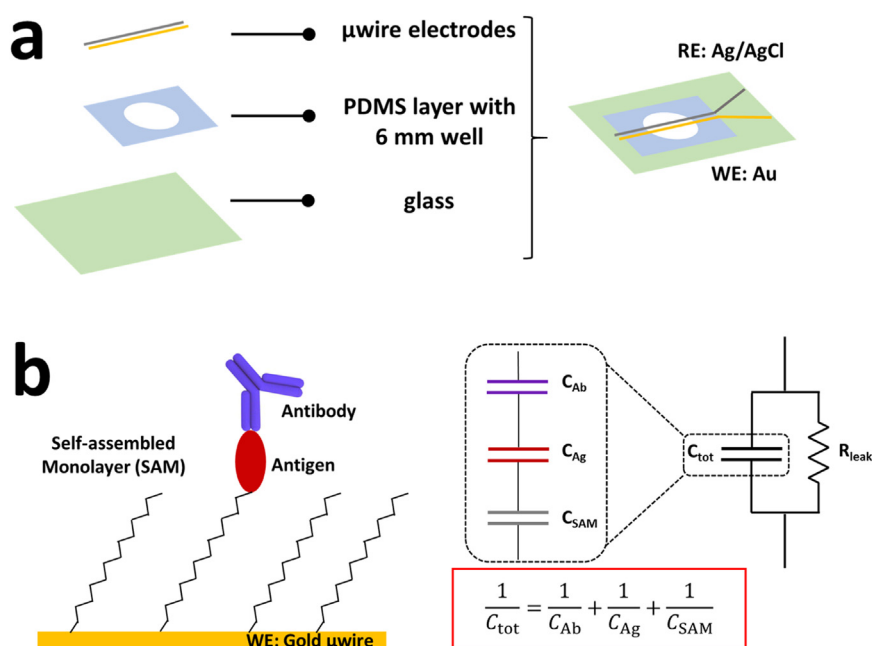


Fig. 1. Schematic of capacitive immunosensor design and working principles. (a) Device layers and resulting immunosensor shown from the top. RE: reference electrode, WE: working electrode; (b) Working electrode (Au microwire) surface chemistry and functionalized layers, with the corresponding equivalent circuit and total capacitance equation. DL capacitance, C_{DL} , is placed in parallel with a leakage resistance, R_{leak} . C_{DL} represents the total capacitance, C_{tot} , of the individual capacitance contribution from each surface layer.

1:10⁶ and 1:10¹² in 30 μ L 1 \times PBST buffer. Following incubation, electrodes were rinsed three times each with 30 μ L 1 \times PBST and 0.1 \times PBST buffer before measurements.

3. Results and discussion

3.1. Sensor design and principles

The label-free capacitive immunosensor introduced here uses microwire electrodes to rapidly and sensitively detect antibodies produced during an immune response, in this case mouse antibodies against ZIKV. The device is comprised of low-cost, easily-acquired materials. A glass slide is used as the base substrate with a polydimethylsiloxane (PDMS) well for sample application. Au and Ag/AgCl microwires (working and reference electrodes, respectively) are immobilized across the PDMS well (Fig. 1a) and 30 μ L of liquid sample is added to the well and incubated for 5 min. Measurements can then be taken in as quickly as one minute. Microelectrode wires, compared to other electrode fabrication methods like ink printing, paste, and sputter-coated electrodes, demonstrate increased mass transport rates due to radial diffusion (Aoki, 1993; Liu et al., 2004). This increases the current density and consequently improves sensitivity and enhances detection limits (Salaün and Van Den Berg, 2006). Microelectrodes offer the additional benefits of simple fabrication without expensive equipment, ease of surface chemical modification, and availability in different pure and alloyed compositions (Adkins and Henry, 2015).

Randle's equivalent circuit is commonly employed to model the electrode-electrolyte interface of a Faradaic biosensor (Marks, 2013). However, our sensor has been designed as a non-Faradaic system to measure capacitive charging currents only. With no offset voltage applied to the electrode, off-target electrochemical reactions or charge transfer at the interface should be minimal. AC electrokinetic microflows have been known to affect capacitive charging currents, but these effects typically begin to occur at a peak-to-peak amplitude of 1–2 V and do not become prominent until 6–15 V (Wu, 2006; Yang and Wu, 2008). The influence of microflows at the 20 mV oscillation voltage used here is negligible. Thus, to model the charging current at the interface, we place C_{DL} in parallel with a leakage resistance, R_{leak} . C_{DL} in turn can be modeled as the total capacitance, C_{tot} , of several capacitors in series, as visualized in Fig. 1b. The first component constitutes the insulating SAM layer on the electrode surface, C_{SAM} . The second, C_{Ag} ,

includes the anchoring groups and the recognition element (antigen), which is followed by the concentration-dependent antibody layer, C_{Ab} .

Based on this model, the binding of antibody to antigen causes a change in the total capacitance, C_{tot} . Because C_{SAM} is constant and does not contribute to capacitive change, the sensitivity of the sensor is predominately determined by the relative capacitance between antigen and antibody. In this case, use of a large analyte such as an antibody increases the sensitivity of our sensor by creating a proportionally larger increase in DL length compared to smaller analytes like antigens (Suni, 2008). This high sensitivity is necessary to adapt the immunosensor for pre-symptomatic pathogen detection, which is currently only achieved by nucleic acid testing (Nicolini et al., 2017).

3.2. Specificity tests and detection limit

To characterize the immunosensor's performance, the ZIKV E-functionalized microwire sensor was first tested with monoclonal antibodies diluted in 1 \times PBST buffer (pH 7.4, 0.05% Tween 20). Anti-ZIKV E (experimental), anti-M13 antibody (control), anti-CHIKV E (control), and anti-DENV antibody (control) were tested (Fig. 2a). Each antibody was applied at concentrations ranging from \sim 1 to \sim 10³ molecules per 30 μ L. The baseline capacitance reading ($C_{Baseline}$) after surface functionalization was directly recorded using an Instek LCR-821 benchtop LCR meter. Capacitance was again directly recorded after target antibody incubation (C_{Ab}). The mean negative capacitance change, $-\Delta C = -(C_{Ab} - C_{Baseline})$, with standard deviation is presented in Fig. 2b for each sample (n = 3). The $-\Delta C$ for anti-ZIKV E is proportional to the concentration/number of antibodies in the experimental sample and can be fit with a regression line ($R^2 = 0.9813$). These results indicate proportionality between the magnitude of the capacitance change and the concentration of the bound target. In comparison, the $-\Delta C$ for controls have no significant change at any tested concentration, suggesting that there was no significant binding between ZIKV E and control antibodies. It is notable that the $-\Delta C$ for the \sim 10 molecule anti-ZIKV E sample is statistically significantly different from the control antibody samples, indicating that the present detection platform has a detection limit as low as \sim 10 antibody molecules per 30 μ L, far superior to that of other immunosensors or ELISA assays (Mattiasson and Hedström, 2016). To demonstrate that the device can be adapted to other antigen/antibody pairs, the sensor was functionalized with CHIKV E2 antigen and tested with the same four

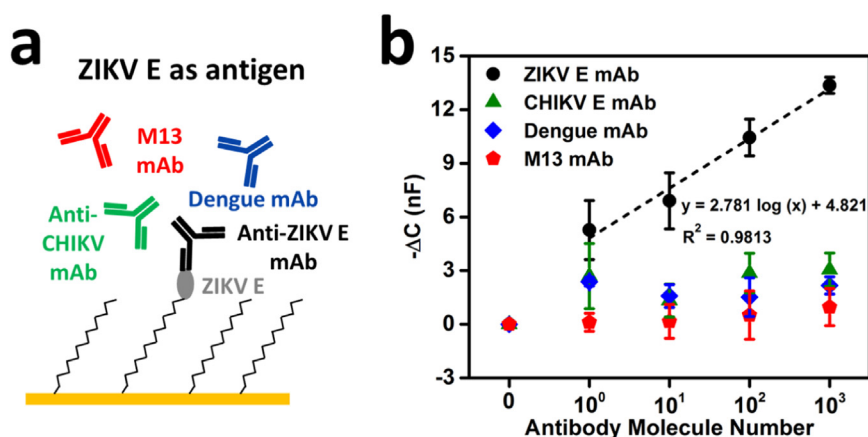


Fig. 2. Specificity tests with monoclonal antibodies. a) Illustration of ZIKV E antigen as the recognition element to test one specific and three nonspecific antibodies; (b) Capacitance responses for the four antibodies at concentrations from 0 to 10^3 molecules per $30 \mu\text{L}$ in $1 \times \text{PBST}$ buffer ($n = 3$ at each concentration, mean \pm STD). The regression fit for specific anti-ZIKV E is shown in the plot as a dashed line.

monoclonal antibodies at the same concentration ranges (Fig. S2).

When normalized for baseline signal variations, the capacitance dropped ~ 7 – 38% for the corresponding dynamic range. Collectively, these results show that the immunosensor functionalized with antigen can selectively capture antibodies at extremely low concentrations without nonspecific binding from other antibodies. This suggests an excellent combination of specificity and sensitivity for this platform. It is unclear what underlying mechanism gives rise to such significant signal changes at low concentrations, but the reported dynamic range was highly reproducible with different antigen-antibody pairs. It is well established that proteins randomly orient themselves when immobilized to a surface (Wu et al., 2008). As a result, binding regions of many probes are not accessible, leaving a portion of the surface inert and causing the active functionalized surface area to be much smaller than the total surface area. Therefore, while ~ 10 antibody molecules may bind to only a small fraction of the total surface area, the proportion of the active surface area that is bound may be significantly larger and may contribute to large percentage changes in capacitance. Although significant advances have been made in the understanding of the interfacial region, thermodynamic models of functionalized surfaces fail when more complex charge distributions are considered (Watkins et al., 2018). Further research is needed to elucidate what is happening at the interface of functionalized surfaces to understand the high sensitivity of our sensing system.

3.3. Isotyping tests with monoclonal antibodies

The isotype of antigen-specific antibodies is commonly determined to elucidate the stage of an infection, with IgM antibodies being present early in infection and IgG antibodies present later. To explore whether our platform could be used to determine isotype, the microwires were functionalized with CHIKV E antigen probe and subsequently saturated with corresponding IgG 2b antibody against CHIKV E ($\sim 10^3$ molecule/ $30 \mu\text{L}$). The capacitance value for anti-CHIKV antibody was set as a new baseline (C_{BL}). The devices were then incubated with six secondary antibodies with different specificities (IgG1, IgG2a, IgG2b, IgG3, IgA and IgM) at concentrations ranging from ~ 1 to $\sim 10^3$ molecules per $30 \mu\text{L}$ (Fig. 3a). Fig. 3b presents the mean negative capacitance changes, $-\Delta C = -(C_{anti-iso Ab} - C_{Baseline})$ with standard deviation for each sample ($n = 3$). As predicted by the circuit model, an additional capacitance change was observed from anti-IgG2b antibody samples in all the concentrations applied. In addition, the $-\Delta C$ of anti-IgG2b antibody increases proportionally with increasing concentrations. In contrast, the five nonspecific anti-isotype antibodies did not increase the capacitance response (Fig. 3b). Supporting previous results of the detection limit, the capacitance of ~ 10 anti-IgG 2b antibody molecules/ $30 \mu\text{L}$ is statistically significantly different from the nonspecific antibodies. These results indicate that our system can accurately determine the isotype of

ultralow concentrations of antigen-specific antibodies.

3.4. Detection of anti-ZIKV antibodies during an immunization time-course

To explore the performance of the capacitive immunosensor in a complex matrix with interfering species, we tested mouse serum for ZIKV-specific polyclonal antibodies. Ten mice were immunized and samples were collected as described in the Supplementary Information. Mouse 3, 4, and 6 samples were tested with the ZIKV E functionalized sensor. Suitable dilutions were determined as described in the Supplementary Information.

Based on the results in Fig S5, two dilutions of the mouse serum, $1:10^6$ and $1:10^{12}$ were chosen for detection for Day 4, 7, 14 and 21 mouse serum samples. Each of the three biological replicates was tested and averaged. Every biological replicate is the average of three technical replicates. The $-\Delta C$ for each post-vaccination sample was compared to the pre-immune sample as shown in Fig. 4a and b. At a $1:10^{12}$ dilution, the $-\Delta C$ increases with each time point after vaccination and saturates around Day 14. The lower $-\Delta C$ for Day 14 can be attributed to its smaller sample size as there was no serum collected for mouse 6 on this day. Although results are similar for the $1:10^6$ dilution compared to the $1:10^{12}$ dilution, it is notable that the $-\Delta C$ for this dilution saturates as early as Day 4 after immunization. Because the $1:10^6$ dilution is significantly more concentrated, this outcome is expected. More importantly, this capacitive immunosensor can detect extremely dilute antibody as early as four days post-vaccination through 21 days. To further characterize the specificity with mouse sera, we examined whether anti-ZIKV serum had any cross-reactivity with CHIKV sensors. The results described in the Supplementary Information (Fig. S4) show reproducibility of the sensor's specificity in a complex physiological matrix.

By reliably detecting as few as 10 molecules and accurately analyzing serum at dilutions of $1:10^{12}$, the results suggest that our sensor has a far superior sensitivity compared to other platforms (Cabral-Miranda et al., 2018; Cecchetto et al., 2017). This increased sensitivity enables us to detect an antibody response four days earlier compared to established serological methods (Jeong et al., 2017). Our sensor also requires less sample volume than comparable ELISAs ($30 \mu\text{L}$ of $1:10^{12}$ vs 50 – $100 \mu\text{L}$ of $1:400$ diluted sample (CDC, 2016)), which preserves precious serum sample and reduces waste. Furthermore, whereas the CDC ZIKV MAC-ELISA needs 12 + hours to obtain results from sample application, our sensor can produce results in under ten minutes. This could result in faster diagnostics needed to determine a timely and effective therapeutic intervention.

3.5. Antibody isotyping of mouse serum samples

Antibody isotyping is a diagnostic component required to separate

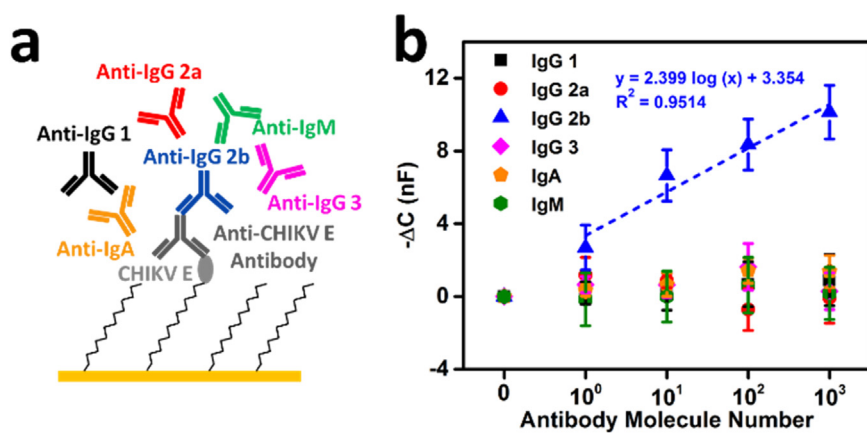


Fig. 3. Isotyping tests with monoclonal antibodies. (a) Illustration of CHIKV E antigen-antibody complex to determine the isotype of anti-CHIKV E (IgG 2b). Six secondary antibodies are used here to perform the test: anti-IgG1, anti-IgG2a, anti-IgG2b, anti-IgG3, anti-IgA and anti-IgM; (b) Capacitance responses of the isotype tests with six secondary antibodies at concentrations from 0 to 10^3 molecules per 30 μL in $1 \times$ PBST buffer ($n = 3$ at each concentration, mean \pm STD). A regression fit is shown in the plot for secondary IgG2b antibody. Similar results were obtained for IgG isotyping of anti-ZIKV monoclonal antibody (Fig. S3).

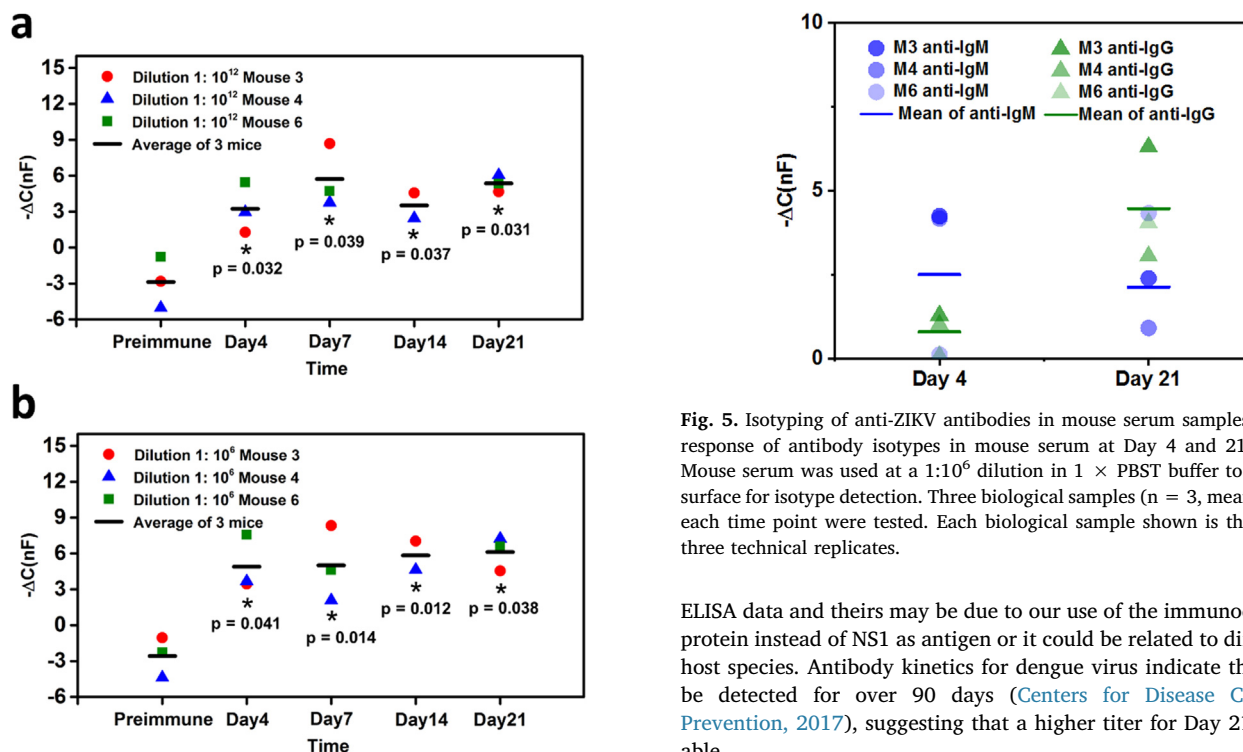


Fig. 4. Immune response kinetics for mouse serum samples. Capacitive response to mouse serum at different time points pre- and post-vaccination with ZIKV. (a) Mouse serum tested at a $1:10^{12}$ dilution in $1 \times$ PBST buffer; (b) Mouse serum tested at a $1:10^6$ dilution in $1 \times$ PBST buffer. Three biological samples ($n = 3$, mean \pm STD) for each time point were tested except for Day 14 ($n = 2$, mean \pm STD). Each biological sample shown is the average of three technique replicates. A paired t -test was carried out between pre- and post-vaccination with ZIKV samples. * paired t -test: $p < 0.05$.

acute from past infections. To characterize whether our sensor platform can be used to determine the isotypes present in a serum sample, wire sensors were functionalized with ZIKV E protein and saturated with serum antibody from Day 4 or Day 21 at a $1:10^6$ dilution. Anti-mouse IgM or IgG was applied to the sensor and the results are compared in Fig. 5. As expected from published flavivirus antibody kinetics (Centers for Disease Control and Prevention, 2017) and the corresponding ELISA data (Fig S6), Day 4 IgM levels were higher than IgG. It was somewhat surprising that the sensor detected constant levels of IgM between Day 4 and Day 21 given that the ELISA showed an increase from Day 4 to Day 21. This may be explained by saturation of the sensor. A recent report, however, indicates that anti-ZIKV IgM levels drop off 8–16 days after symptom onset (Jeong et al., 2017). The discrepancy between our

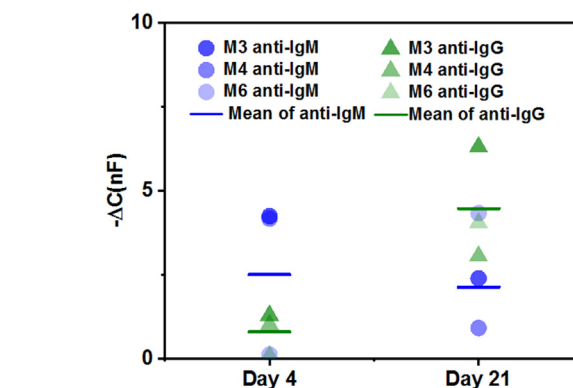


Fig. 5. Isotyping of anti-ZIKV antibodies in mouse serum samples. Capacitive response of antibody isotypes in mouse serum at Day 4 and 21 with ZIKV. Mouse serum was used at a $1:10^6$ dilution in $1 \times$ PBST buffer to saturate the surface for isotype detection. Three biological samples ($n = 3$, mean \pm STD) for each time point were tested. Each biological sample shown is the average of three technical replicates.

ELISA data and theirs may be due to our use of the immunodominant E protein instead of NS1 as antigen or it could be related to differences in host species. Antibody kinetics for dengue virus indicate that IgM can be detected for over 90 days (Centers for Disease Control and Prevention, 2017), suggesting that a higher titer for Day 21 is reasonable.

The sensor results also show an increase in IgG levels from Day 4 to Day 21, which agrees with the ELISA data. The sensor also shows higher IgG levels on Day 21 compared to IgM. These data conflict with the ELISA results, which show slightly higher IgM for both days. However, the ELISA assays in Fig. S4 were performed at $1:100$ dilution, which was the highest dilution that gave detectable anti-ZIKV signals. We hypothesize that matrix effects in these concentrated mouse sera likely affected apparent antibody isotype distributions in the ELISA assays. Also, because the IgM is significantly larger than IgG, steric hindrance may cause the IgM sensor to saturate faster than the IgG sensor. As a smaller molecule, more IgG may be able to bind to the wire surface and produce a larger signal. Cabral-Miranda et al. recently published an immunosensor for ZIKV antibody with isotyping capacity that was able to detect a 10^6 to 10^7 dilution of serum (Cabral-Miranda et al., 2018). However, their design has decreased sensitivity compared to our system and it also incorporates a toxic redox couple that limits its POC use. Without using labels or redox couples, our sensor can distinguish antibody isotypes from a complex serum matrix containing a mixture of isotypes. These results enhance the applicability of the sensor for POC diagnosis and even for research purposes.

4. Conclusions

Diagnosis of infectious diseases like ZIKV requires laboratory confirmation but current methodologies are limited to use by specialized diagnostic laboratories. Recent outbreaks like that of Ebola virus and ZIKV indicate a growing need for simple, sensitive, and selective diagnostics amenable to a POC setting. The ultra-sensitive capacitance sensor introduced in this study represents a simple and robust platform for antibody detection in serum. Within minutes, it can detect as few as ~10 antibody molecules in a 30 μ L volume and determine their isotype. Without using labels or redox couples, our sensor can detect anti-ZIKV antibodies during an immunization time course and distinguish the isotype from a complex serum matrix. Furthermore, this sensor design can be easily integrated with microfluidics and handheld measuring devices to make it suitable for field work and POC testing. Our research team is currently working to integrate this immunosensor platform into our previously developed paper-based analytical device (Channon et al., 2018). Continued development of this novel platform can greatly increase the capacity of public health agencies worldwide to assess drug or vaccine efficacy and to monitor emerging infectious diseases of global importance in future.

Acknowledgements

This work was funded by NSF 1332404 to D.S.D. and NIH NIAID 1R01AI114675 and 1R01AI132668 to B.J.G. The work reported here was also partially supported by a National Science Foundation grant (DGE-1450032). Any opinions, findings, conclusions or recommendations expressed are those of the authors and do not necessarily reflect the views of the National Science Foundation. We would like to thank Mr. Benjamin Fuller, Dr. Dick Bowen, Dr. Michael Diamond for providing assistance and reagents.

Declaration-of-competing-interests

None.

Appendix A. Supplementary material

Supplementary data associated with this article can be found in the online version at <https://doi.org/10.1016/j.bios.2019.01.040>.

References

- Adkins, J.A., Henry, C.S., 2015. Electrochemical detection in paper-based analytical devices using microwire electrodes. *Anal. Chim. Acta* 891, 247–254. <https://doi.org/10.1016/j.aca.2015.07.019>.
- Adornetto, G., Fabiani, L., Volpe, G., De Stefano, A., Martini, S., Nenna, R., Lucantoni, F., Bonamico, M., Tiberti, C., Moscone, D., 2015. An electrochemical immunoassay for the screening of celiac disease in saliva samples. *Anal. Bioanal. Chem.* 407, 7189–7196. <https://doi.org/10.1007/s00216-015-8884-y>.
- Aoki, K., 1993. Theory of ultramicroelectrodes. *Electroanalysis* 5, 627–639. <https://doi.org/10.1002/elan.1140050802>.
- Baden, L.R., Petersen, L.R., Jamieson, D.J., Powers, A.M., Honein, M.A., 2016. Zika Virus. *N. Engl. J. Med.* NEJMra 1602113. <https://doi.org/10.1056/NEJMra1602113>.
- Berggren, C., Bjarnason, B., Johansson, G., 2001. Capacitive biosensors. *Electroanalysis* 13, 173–180. [https://doi.org/10.1002/1521-4109\(200103\)13:3<173::AID-ELAN173>3.0.CO;2-B](https://doi.org/10.1002/1521-4109(200103)13:3<173::AID-ELAN173>3.0.CO;2-B).
- Cabral-Miranda, G., Cardoso, A.R., Ferreira, L.C.S., Sales, M.G.F., Bachmann, M.F., 2018. Biosensor-based selective detection of Zika virus specific antibodies in infected individuals. *Biosens. Bioelectron.* 113, 101–107. <https://doi.org/10.1016/j.bios.2018.04.058>.
- Carteaux, G., Maquart, M., Bedet, A., Contou, D., Brugières, P., Fourati, S., Cleret de Langavant, L., de Broucker, T., Brun-Buisson, C., Leparco-Goffart, I., Mekontso Dessap, A., 2016. Zika Virus Associated with Meningoencephalitis. *N. Engl. J. Med.* 375, 1386–1388. <https://doi.org/10.1056/NEJMcl1602964>.
- CDC, 2016. Zika MAC-ELISA For Use Under an Emergency Use.
- Cecchetto, J., Fernandes, F.C.B., Lopes, R., Bueno, P.R., 2017. The capacitive sensing of NS1 flavivirus biomarker. *Biosens. Bioelectron.* 87, 949–956. <https://doi.org/10.1016/j.bios.2016.08.097>.
- Centers for Disease Control and Prevention, 2017. Laboratory Guidance and Diagnostic Testing [WWW Document]. URL <<https://www.cdc.gov/dengue/clinicalab/laboratory.html>> (accessed 9 October 2018).
- Channon, R.B., Yang, Y., Feibelman, K.M., Geiss, B.J., Dandy, D.S., Henry, C.S., 2018. Development of an electrochemical paper-based analytical device for trace detection of virus particles. *Anal. Chem.* 90, 7777–7783. <https://doi.org/10.1021/acs.analchem.8b02042>.
- Crowther, J.R., 2008. The ELISA Guidebook Series Editor.
- Ertürk, G., Mattiasson, B., 2017. Capacitive biosensors and molecularly imprinted electrodes. *Sens. (Switz.)* 17, 1–21. <https://doi.org/10.3390/s17020390>.
- Jeong, Y.E., Cha, G.W., Cho, J.E., Lee, E.J., Jee, Y., Lee, W.J., 2017. Viral and serological kinetics in Zika virus-infected patients in South Korea. *Virology* 14, 4–9. <https://doi.org/10.1186/s12985-017-0740-6>.
- Leal, M.C., Muniz, L.F., Ferreira, T.S.A., Santos, C.M., Almeida, L.C., Linden, V., Der, Van, Ramos, R.C.F., Rodrigues, L.C., Caldas Neto, S.S., 2016. Hearing Loss in Infants with Microcephaly and Evidence of Congenital Zika Virus Infection — Brazil, November 2015 – May 2016. *MMWR Morb Mortal Wkly Rep* 65, pp. 2015–2017. <https://doi.org/10.15585/mmwr.mm6534e3>.
- Liu, Y., Vickers, J.A., Henry, C.S., 2004. Simple and sensitive electrode design for microchip electrophoresis/electrochemistry. *Anal. Chem.* 76, 1513–1517. <https://doi.org/10.1021/ac0350357>.
- Loyprasert, S., Hedström, M., Thavarungkul, P., Kanatharana, P., Mattiasson, B., 2010. Sub-attomolar detection of cholera toxin using a label-free capacitive immunosensor. *Biosens. Bioelectron.* 25, 1977–1983. <https://doi.org/10.1016/j.bios.2010.01.020>.
- Marks, R.S., 2013. *Electrochemical Biosensors*. Taylor & Francis Group, LLC, Boca Raton, FL.
- Mattiasson, B., Hedström, M., 2016. Capacitive biosensors for ultra-sensitive assays. *TrAC - Trends Anal. Chem.* 79, 233–238. <https://doi.org/10.1016/j.trac.2015.10.016>.
- Mécharles, S., Herrmann, C., Poullain, P., Tran, T., Deschamps, N., Mathon, G., Landais, A., Breurec, S., 2016. Case report acute myelitis due to Zika virus infection. *Lancet* 8, 6736. <https://doi.org/10.1136/bcr-2012-007094.4>.
- Miner, J.J., Cao, B., Govero, J., Smith, A.M., Fernandez, E., Cabrera, O.H., Garber, C., Noll, M., Klein, R.S., Noguchi, K.K., Mysorekar, I.U., Diamond, M.S., 2016. Zika Virus Infection during Pregnancy in Mice Causes Placental Damage and Fetal Demise. *Cell* 165, 1081–1091. <https://doi.org/10.1016/j.cell.2016.05.008>.
- Mlakar, J., Korva, M., Tul, N., Popović, M., Poljšak-Prijatelj, M., Mraz, J., Kolenc, M., Resman Rus, K., Vesnaver Vipotnik, T., Fabjan Vodusek, V., Vizjak, A., Pizem, J., Petrovec, M., Avšič Županc, T., 2016. Zika virus associated with microcephaly (160210140106006). *N. Engl. J. Med.* <https://doi.org/10.1056/NEJMoa1600651>.
- Nicolini, A.M., McCracken, K.E., Yoon, J.-Y., 2017. Future developments in biosensors for field-ready Zika virus diagnostics. *J. Biol. Eng.* 11, 7. <https://doi.org/10.1186/s13036-016-0046-z>.
- Oehler, E., Watrin, L., Larre, P., Leparco-Goffart, I., Lastere, S., Valour, F., Baudouin, L., Mallet, H., Musso, D., Ghawche, F., 2014. Zika virus infection complicated by Guillain-Barre syndrome—case report, French Polynesia, December 2013. *Euro Surveill* 19, pp. 7–9. <https://doi.org/10.2807/1560-7917.ES2014.19.9.20720>.
- Pierson, T.C., Sánchez, M.D., Puffer, B.A., Ahmed, A.A., Geiss, B.J., Valentine, L.E., Altamura, L.A., Diamond, M.S., Doms, R.W., 2006. A rapid and quantitative assay for measuring antibody-mediated neutralization of West Nile virus infection. *Virology* 346, 53–65. <https://doi.org/10.1016/j.virol.2005.10.030>.
- Posthuma-Trumpie, G.A., Korf, J., Van Amerongen, A., 2009. Lateral flow (immuno) assay: its strengths, weaknesses, opportunities and threats. A literature survey. *Anal. Bioanal. Chem.* 393, 569–582. <https://doi.org/10.1007/s00216-008-2287-2>.
- Prado, I.C., Chino, M.E.T.A., dos Santos, A.L., Souza, A.L.A., Pinho, L.G., Lemos, E.R.S., De-Simone, S.G., 2018. Development of an electrochemical immunosensor for the diagnostic testing of spotted fever using synthetic peptides. *Biosens. Bioelectron.* 100, 115–121. <https://doi.org/10.1016/j.bios.2017.08.029>.
- Rabe, I.B., Staples, J.E., Villanueva, J., Hummel, K.B., Johnson, J.A., Rose, L., Hills, S., Wasley, A., Fischer, M., Powers, A.M., 2016. Interim Guidance for Interpretation of Zika Virus Antibody Test Results. *Mmwr. Morb. Mortal. Wkly. Rep.* 65, 543–546. <https://doi.org/10.15585/mmwr.mm6521e1>.
- Salaün, P., Van Den Berg, C.M.G., 2006. Voltammetric detection of mercury and copper in seawater using a gold microwire electrode. *Anal. Chem.* 78, 5052–5060. <https://doi.org/10.1021/ac060231+>.
- Soares, C.N., Brasil, P., Medialdea, R., Msc, C., Sequeira, P., Bispo De Filippis, A., Borges, V.A., Theophilo, F., Ellul, M.A., Tom, M., Frp, S., 2016. Fatal encephalitis associated with Zika virus infection in an adult. *J. Clin. Virol.* 83, 63–65. <https://doi.org/10.1016/j.jcv.2016.08.297>.
- Suni, I.I., 2008. Impedance methods for electrochemical sensors using nanomaterials. *TrAC - Trends Anal. Chem.* 27, 604–611. <https://doi.org/10.1016/j.trac.2008.03.012>.
- van der Eijk, A.A., van Genderen, P.J., Verdijk, R.M., Reusken, C.B., Mögling, R., van Kampen, J.J.A., Widagdo, W., Aron, G.I., GeurtsvanKessel, C.H., Pas, S.D., Raj, V.S., Haagmans, B.L., Koopmans, M.P.G., 2016. Miscarriage associated with Zika virus infection. *N. Engl. J. Med.* 375, 1386–1388. <https://doi.org/10.1056/NEJMcl1605898>.
- Ventura, L.O., Ventura, C.V., Lawrence, L., van der Linden, V., van der Linden, A., Gois, A.L., Cavalcanti, M.M., Barros, E.A., Dias, N.C., Berrocal, A.M., Miller, M.T., 2017. Visual impairment in children with congenital Zika syndrome (<https://doi.org/10.1016/j.jaapos.2017.04.003>). *J. Am. Assoc. Pediatr. Ophthalmol. Strabismus*. <https://doi.org/10.1016/j.jaapos.2017.04.003>.
- Ventura, C.V., Maia, M., Bravo-Filho, V., Gois, A.L., Belfort, R., 2016. Zika virus in Brazil and macular atrophy in a child with microcephaly. *Lancet* 387, 228. [https://doi.org/10.1016/S0140-6736\(16\)00006-4](https://doi.org/10.1016/S0140-6736(16)00006-4).
- Wang, L., Veselinovic, M., Yang, L., Geiss, B.J., Dandy, D.S., Chen, T., 2016. A sensitive DNA capacitive biosensor using interdigitated electrodes. *Biosens. Bioelectron.* 87, 646–653. <https://doi.org/10.1016/j.bios.2016.09.006>.
- Watkins, H.M., Ricci, F., Plaxco, K.W., 2018. Experimental Measurement of Surface Charge Effects on the Stability of a Surface-Bound Biopolymer. *Langmuir* acc.

- Langmuir. 8 b01004. <https://doi.org/10.1021/acs.langmuir.8b01004>.
- Wu, J., 2006. Biased AC electro-osmosis for on-chip bioparticle processing. IEEE Trans. Nanotechnol. 5, 84–88. <https://doi.org/10.1109/TNANO.2006.869645>.
- Wu, P., Castner, D.G., Grainger, D.W., 2008. Diagnostic devices as biomaterials: a review of nucleic acid and protein microarray surface performance issues. J. Biomater. Sci. Polym. Ed. 19, 725–753. <https://doi.org/10.1163/156856208784522092>.
- Yang, K., Wu, J., 2008. Investigation of microflow reversal by ac electrokinetics in orthogonal electrodes for micropump design. Biomicrofluidics 2, 1–8. <https://doi.org/10.1063/1.2908026>.